

# Development of the Cybernetic Shoulder – A Three DOF Mechanism that Imitates Biological Shoulder-Motion –

Masafumi OKADA\*<sup>1</sup>, Yoshihiko NAKAMURA\*<sup>1\*2</sup> and Shin-ichiro HOSHINO\*<sup>1</sup>

\*<sup>1</sup>Dept. of Mechano-Informatics, Univ. of Tokyo  
7-3-1 Hongo Bunkyo-ku Tokyo, 113 Japan

\*<sup>2</sup>The CREST Program the Japan Science and Technology Corporation  
e-mail : okada@ynl.t.u-tokyo.ac.jp

## Abstract

*In this paper, we discuss the integration of "mechanical softness" into the humanoid robot mechanisms design. The mechanical softness include such requirements as human-like high mobility and human-like sensitive compliance. We focus on the shoulder mechanism in this paper, and propose a new parallel mechanism to integrate the two requirements. The mechanism is named the Cybernetic Shoulder and possesses three degrees-of-freedom. The nature of motion curves of human shoulder, and the design and development of the cybernetic shoulder are to be described with the computation issue of kinematics. The integration of compliance into the parallel mechanism is also discussed, and its experimental evaluation is made.*

## 1 Introduction

As the research of humanoid robots goes on [1]~[4] and their application are discussed with reality, the importance of "mechanical softness" grows its importance. The mechanical softness ambiguously represents the hope that the physical presence of a humanoid robot among humans is naturally acceptable. The requirements for mechanical softness are wide, but would certainly include (1) human-like high mobility and (2) human-like sensitive compliance. The present paper develops the idea of integration of mechanical softness, in particular, for humanoid shoulder.

**Human-like mobility** is demanded from the same reasons that demand the human-like geometry for a humanoid being in the human-structured environments. Furthermore, being among humans a hu-

manoid is required to move with smooth and natural curves that we show using high degrees-of-freedom mobility. It is important from the geometric functionality point of view and psychological one well. This requirement is contradict with one for mechanical simplicity from the implementation point of view and, therefore, poses an important design problem.

**Human-like sensitive compliance** is closely linked with the safety issue when a humanoid is among humans not only with the functionality in the human-structured environments. Contacts, collisions and stability with their presence require a special attention for a humanoid robot. The technical discussions need to be elaborated on what kind of compliance to be integrated in a humanoid and how to implement it in the mechanism.

In this paper, we first see the mechanism of human shoulder and learn the nature of curves of shoulder motion. The cybernetic shoulder is, then, proposed, designed and prototyped taking an advantage of parallel mechanism. Mathematics to solve the kinematics is also developed and coded for real-time control. Section 5 describes our approaches and efforts to integrate human-like sensitive compliance by adopting elastic and damping mechanical components as parts of the parallel mechanism. The experimental evaluation is also provided.

## 2 Human Shoulder Mechanism

Figure 1 shows the human shoulder mechanism. The human shoulder is composed by 5 joints that are split into two groups. One is a shoulder part (joint *A* and *B*), the other is a chest part (*C*, *D* and *E*). These joints move dependently in each groups so that the hu-

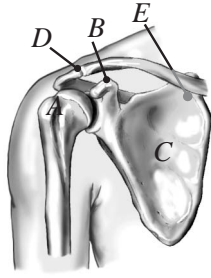


Figure 1: Human shoulder mechanism (quoted from Media Crip.)

man shoulder can move smoothly [5]. Figure 2 shows the motion of the human shoulder. This figure shows that the human shoulder's motion does not have a fixed center of rotation. We consider that causes the

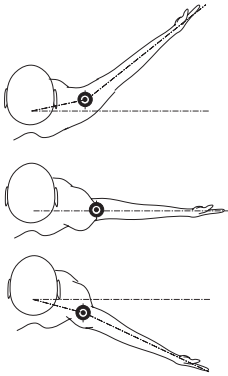


Figure 2: Motion of the human shoulder

human-like motion. The conventional design of anthropomorphic seven degrees-of-freedom manipulators cannot realize this motion.

### 3 Mechanism of the Cybernetic Shoulder

Figure 3 shows the model of the cybernetic shoulder, where  $\beta$  and  $\delta$  are two degrees-of-freedom gimbal mechanisms,  $d$  is a three degrees-of-freedom ball joint,  $b$  is a two degrees-of-freedom universal joint,  $a$  is a four degrees-of-freedom joint of spherical and prismatic motion, and  $e$  is a prismatic joint. Moving point  $A$  within vertical plane alters the pointing direction of the main shaft  $G$ , which determines, along with the

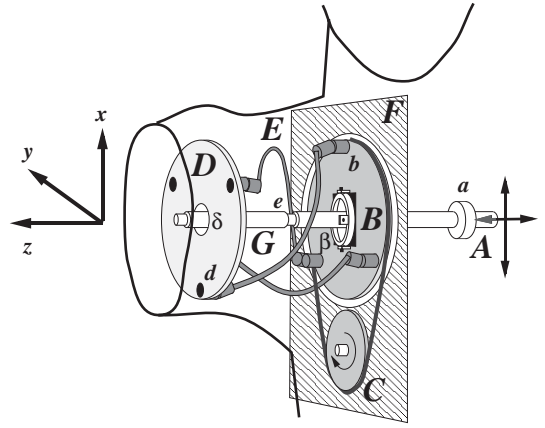


Figure 3: Cybernetic shoulder

constraints due to the free curved links  $E$  between points  $b$  and  $d$ , the direction of the normal vector of  $D$ . The rotation about the normal of  $D$  is mainly determined by the rotation of  $C$  through  $B$  and  $G$ . Note that the rotation of  $C$  is coupled with the pointing direction of  $D$  when  $B$  and  $D$  are not parallel. The advantages of this mechanism are summarized as follows:

**Compactness** Since the cybernetic shoulder can locate its actuators inside the chest, the shoulder geometry occupies rather small volume and shows a smooth shape, compared with conventional designs of shoulder joints of manipulators.

**Large workspace** Figure 4 shows the motion of the cybernetic shoulder, in the reduced two dimensional model. When the main shaft  $G$  rotates  $\psi$

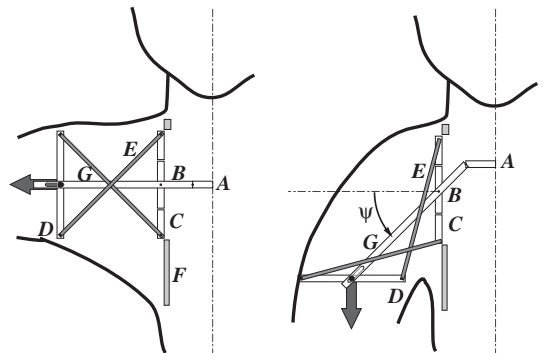


Figure 4: Motion of the Cybernetic Shoulder

within  $\pm 45$  degree, the normal vector of  $D$  rotates within nearly twice as much  $\pm 90$  degree.

Although this magnification ratio is not constant, it generates a large workspace.

**Human-like motion** Figure 5 shows a locus of centers of rotation when point  $A$  moves along  $y$  axis. This figure shows a distinctive charac-

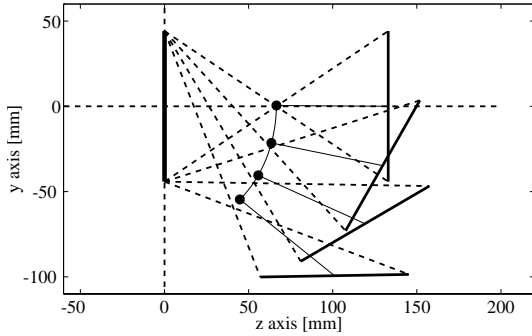


Figure 5: Center of rotation

teristics that the center of rotation of the cybernetic shoulder makes a similar motion to that of the human shoulder motion as seen in Figure 2. The authors would like to claim that the cybernetic shoulder generates with the reduced three degrees-of-freedom mechanism. The natural and smooth motions that the human shoulder does with higher degrees-of-freedom and higher mechanical complexity.

**Singularity Free** The theoretical range of the rotation of link  $G$  is  $|\psi| < 90$  degree, and  $\psi = \pm 90$  degrees implies singular points. In practice, mechanical design limits the range of  $\psi$  a bit smaller. Although the upper limit of  $\psi$  depends on the rotation of plate  $B$  about the  $z$  axis, the range of  $\psi$  of the prototype spans  $\pm 45$  degrees regardless of the rotation. This range of  $\psi$  enables the normal of plate  $D$  to span those of a semisphere. This workspace is larger than that of the typical shoulders of conventional design.

**Small Backlash** The cybernetic shoulder has a double universal-joint structure which yields a human shoulder geometry and has a human like motion. Many types of double universal-joint structures have already been reported [3, 6, 7], where the double universal-joint mechanisms were commonly driven by gears and, therefore, unfortunately suffer from large backlash. On the other hand, the constraints of the cybernetic shoulder

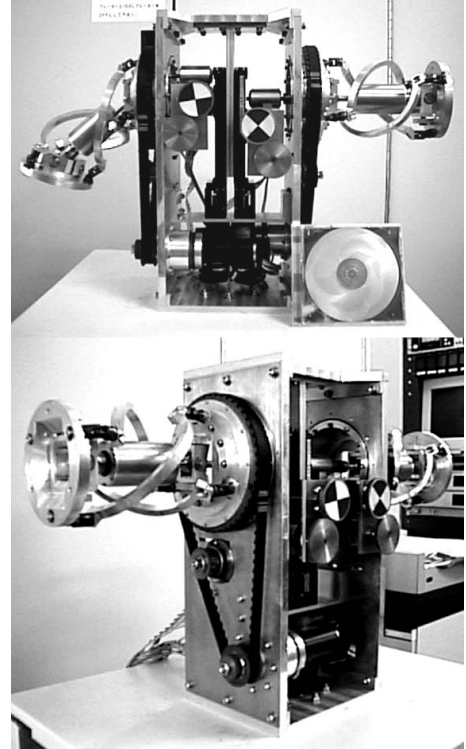


Figure 6: Photographs of the cybernetic shoulder

are provided by closed kinematic chains and realize rather small backlash.

Figures 6 and 7 show photographs of the prototyped cybernetic shoulder. The body is about 400mm high, and about 600mm wide between the end of the left shoulder and right shoulder. The diameter of plate  $D$  is approximately 110mm. The three degrees-of-freedom are directed by three DC motors of 90W. The planner motion of point  $A$  is made by two perpendicular ball-screw axes assembled in series.

## 4 Kinematics of the cybernetic shoulder

Due to the complexity of a closed kinematic chain, There is no closed form solution of inverse or forward kinematics. We, therefore, developed a numerical method to solve the kinematics.

We define parameters and coordinate systems as shown in Figure 8.  $x_0y_0z_0$  is the absolute coordinate system with the origin at the  $\beta$ , center of  $B$ .  $x_1y_1z_1$  is the end plate coordinate system with the origin at the

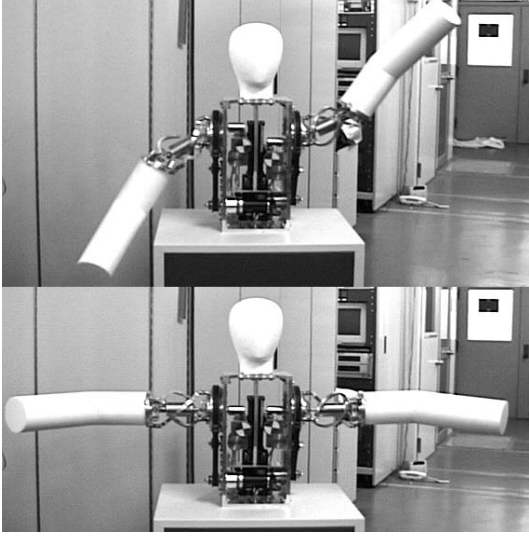


Figure 7: Motion of the experimental system

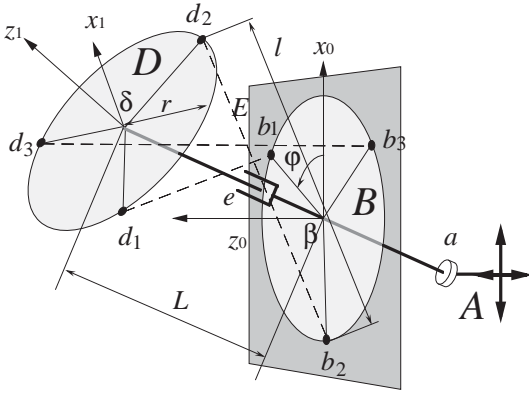


Figure 8: Model of the cybernetic shoulder

$\delta$ , center of  $D$ . The rotation of plate  $B$  is measured from  $x_0$  axis and takes zero degree when  $\mathbf{b}_1$  has the same direction as  $x_0$ . In Figure 8, plate  $B$  is rotated  $\phi$  about the  $z_0$  axis. In the following,  $[\cdot]^i$  means a vector in the  $x_i y_i z_i$  coordinate system and  $\mathbf{R}_\theta^\xi$  implies the rotation of  $\theta$  about the  $\xi$  axis. Accordingly,

$$\mathbf{b}_i^0 = \mathbf{R}_\phi^{z_0} \mathbf{R}_{\frac{2}{3}(i-1)\pi}^{z_0} [r \ 0 \ 0]^T \quad (1)$$

$$\mathbf{d}_i^1 = \mathbf{R}_{\frac{2}{3}(i-1)\pi}^{z_0} [r \ 0 \ 0]^T \quad (2)$$

are satisfied. Since  $\beta$  and  $\delta$  have gimbal mechanisms, we consider  $\theta_{x0}$ , the rotation about the  $x_0$  axis,  $\theta_{y0}$ , the rotation about the  $y_0$  axis,  $\theta_{y1}$ , the rotation about the  $y_1$  axis, and  $\theta_{x1}$ , the rotation about the  $x_1$  axis in order like an euler angle coordinates. We then obtain

the following equations:

$$\mathbf{d}_i^0 = \delta + \mathbf{R} \mathbf{d}_i^1 \quad (i = 1, 2, 3) \quad (3)$$

$$\delta := L \mathbf{R}_A \mathbf{e}_z \quad (4)$$

$$\mathbf{R} := \mathbf{R}_A \mathbf{R}_B \quad (5)$$

$$\mathbf{R}_A := \mathbf{R}_{\theta_{x0}}^{x_0} \mathbf{R}_{\theta_{y0}}^{y_0} \quad (6)$$

$$\mathbf{R}_B := \mathbf{R}_{\theta_{y1}}^{y_1} \mathbf{R}_{\theta_{x1}}^{x_1} \mathbf{R}_\pi^{z_1} \quad (7)$$

$$\mathbf{e}_z = [0 \ 0 \ 1]^T \quad (8)$$

where  $\theta_{x0}, \theta_{y0}$  and  $\phi$  are determined by the position of  $A$  and the rotation angle of  $B$ . Variables such as  $\theta_{x1}, \theta_{y1}$  and  $L$  are to be computed. From the kinematic constraints of that the lengths of link  $E$  are constant, we have

$$|\mathbf{d}_i^0 - \mathbf{b}_i^0| = \ell \quad (9)$$

From equation (3), the above equation is written as follows:

$$|L \mathbf{R}_A \mathbf{e}_z + \mathbf{R} \mathbf{d}_i^1 - \mathbf{b}_i^0| = \ell_i \quad (10)$$

To solve this equation, we apply numerical computation. We set the cost function  $J$  as follows:

$$J = \sum_{i=1}^3 J_i^2 \quad (11)$$

$$J_i := |\mathbf{R}_A \mathbf{e}_z + \mathbf{R} \mathbf{d}_i^1 - \mathbf{b}_i^0| - \ell_i \quad (i = 1, 2, 3) \quad (12)$$

Defining  $T_{\theta_{x1}}$  and  $T_{\theta_{y1}}$  as

$$T_{\theta_{x1}} := \tan \frac{\theta_{x1}}{2} \quad (13)$$

$$T_{\theta_{y1}} := \tan \frac{\theta_{y1}}{2} \quad (14)$$

we iteratively calculate

$$T_{\theta_{x1}} = T_{\theta_{x1}} - k_1 \frac{\partial J}{\partial T_{\theta_{x1}}} \quad (15)$$

$$T_{\theta_{y1}} = T_{\theta_{y1}} - k_2 \frac{\partial J}{\partial T_{\theta_{y1}}} \quad (16)$$

$$L = L - k_3 \frac{\partial J}{\partial L} \quad (17)$$

where  $k_1, k_2, k_3$  are constant and  $\frac{\partial J}{\partial T_{\theta_{x1}}}, \frac{\partial J}{\partial T_{\theta_{y1}}}, \frac{\partial J}{\partial L}$  are given by

$$\frac{\partial J}{\partial s} = 2 \sum_{i=1}^3 \frac{\partial J_i}{\partial s} J_i \quad (s = T_{\theta_{x1}}, T_{\theta_{y1}}, L) \quad (18)$$

$$\frac{\partial J_i}{\partial L} = |\mathbf{R}_A \mathbf{e}_z| \quad (19)$$

$$\frac{\partial J_i}{\partial T_{\theta_{x1}}} = \left| L \frac{\partial \mathbf{R}_A}{\partial T_{\theta_{x1}}} e_z + \frac{\partial \mathbf{R}}{\partial T_{\theta_{x1}}} d_i^1 \right| \quad (20)$$

$$\frac{\partial J_i}{\partial T_{\theta_{y1}}} = \left| L \frac{\partial \mathbf{R}_A}{\partial T_{\theta_{y1}}} e_z + \frac{\partial \mathbf{R}}{\partial T_{\theta_{y1}}} d_i^1 \right| \quad (21)$$

using  $\theta_{x0}$ ,  $\theta_{y0}$  and current values of  $\theta_{x1}$ ,  $\theta_{y1}$  and  $L$ . We verified that the cost function  $J$  converged to zero with the accuracy of  $\pm 2\%$  for small movements of the orientation of the end plate within 10 times iterations. By using reference motor rotation angles obtained by the above computation, each motors are controlled by PD controller.

## 5 Passive Compliance

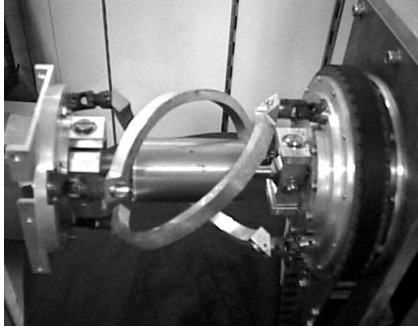


Figure 9: Cybernetic Shoulder with rigid link

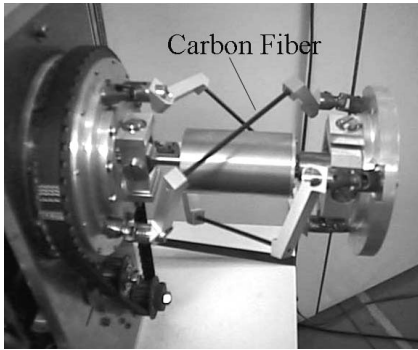


Figure 10: Cybernetic Shoulder with carbon fiber link

A humanoid robot requires mechanical softness so as not to injure the humans sharing the common space. Using the closed kinematic chain of the cybernetic shoulder, we can design and integrate the softness of mechanism. The compliance of the cybernetic shoulder can be realized by properly designing parameters

of link  $E$  in Figure 3. We would like to show a few examples of such implementation.

Figure 9 shows the link  $E$  using the original rigid material of aluminum alloy (Type 1). As an attempt to implement passive compliance, a thin carbon fiber ( $\phi 3\text{mm}$ ) rod is used as an elastic material in Figure 10 (Type 2). The shape of this link is shown in Figure 11. As shown later, this link had large compliance and small damping. To improve the characteristics, we designed the third link. Figure 12 shows the

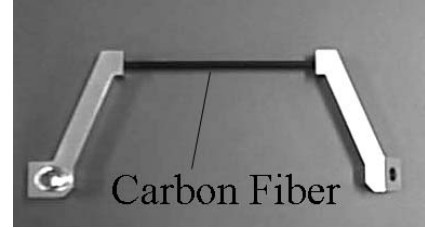


Figure 11: A prototype of the link  $E$

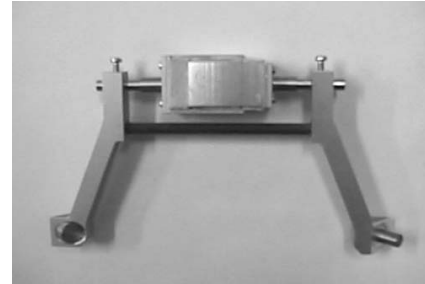


Figure 12: Link  $E$  with a damper

Table 1: Spring constant and coefficient of viscosity

Type	Spring constant (N/m)	Coefficient of viscosity (kg/s)
1	$1.609 \times 10^3$	0.625
2	$1.485 \times 10^2$	0.660
3	$5.963 \times 10^2$	1.05

$\phi 5\text{mm}$  carbon fiber link with a damper (Type 3). The damper is designed as shown in Figure 13 using Temper Foam<sup>1</sup>. The spring constant and the coefficient of

<sup>1</sup>Temper Foam : Produced by EAR SPECIALITY COMPOSITES Corp. shows frequency dependent characteristics. Namely, it shows high stiffness for high frequency, high viscosity for low frequency.

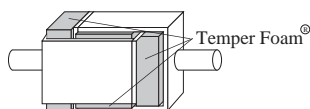


Figure 13: Design of a damper

viscosity of the three type of links are shown in Table 1. By using carbon rods, mechanical softness is realized. The impulse responses of the end plate of the cybernetic shoulder using  $\phi 3\text{mm}$  carbon link (Type 2) and the  $\phi 5\text{mm}$  carbon link with damper (Type 3) are shown in Figure 14, where magnitudes of the initial

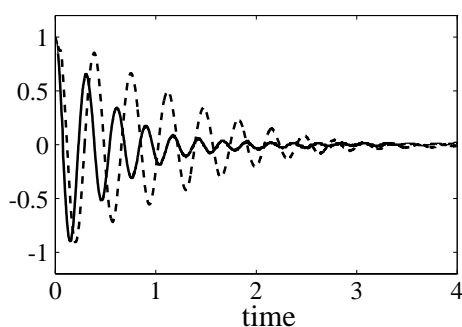


Figure 14: Impulse responses (Dashed line : Type 2, Solid line : Type3)

conditions are normalized. The designed damper has large effectiveness for the viscosity of the cybernetic shoulder.

For the precision and ease of control, high stiffness is suitable, while the safety consideration requires low stiffness. To technically compromise these two conflicting requirements, we may require a nonlinear elasticity. An example of such elasticity is one known for the TiNi shape memory alloy (SMA). When the strain is large, the maximum stress are limited. It is also known that elasticity and viscosity can be controlled by changing temperature of SMA. Adopting SMA as link material can be a promising approach to integrate a safety of the humanoid robot. This will be one of our future problem.

## 6 Conclusions

In this paper, we have proposed, designed and fabricated the new mechanism cybernetic shoulder for the

humanoid robot shoulder.

1. The advantages of the cybernetic shoulder are compactness, large mobile area, human-like motion, singularity free and small backlash. And because of the closed kinematic chain, it is easy to introduce the human like compliance to the cybernetic shoulder.
2. We have developed mathematics to solve the kinematics of the cybernetic shoulder.
3. We can design the elasticity and the viscosity of the cybernetic shoulder by changing the material of link  $E$  which determines the kinematic constraints.
4. We have designed two types of new link  $E$ . One is  $\phi 3\text{mm}$  carbon fiber link which has large compliance and small damping. The other is  $\phi 5\text{mm}$  carbon fiber link with a damper using Temper Form. The latter link has appropriate large compliance and damping for humanoid robots.

This research was supported by the Research for the Future Program, the Japan Society for the Promotion of Science (Project No. JSPS-RFTF96P00801).

## References

- [1] J.Yamaguchi and A.Takanishi: Development of a Biped Walking Robot Having Antagonistic Driven Joints Using Nonlinear Spring Mechanism; Proc. of the IEEE International Conference on Robotics and Automation, pp. 185-192 (1997)
- [2] K.Hirai, M.Hirose, Y.Haikawa and T.Takenaka: The Development of Honda Humanoid Robot; Proc. of the IEEE International Conference on Robotics and Automation, pp. 1321-1326 (1997)
- [3] M.E.Rosheim: Robot Evolution, The Development of Anthrobotics; JOHN & SONS, INC. (1994)
- [4] M.Inaba, T.Ninomiya, Y.Hoshino, K.Nagasaka, S.Kagami and H.Inoue: A Remote-Brain Full-Body Humanoid with Multisensor Imaging System of Binocular Viewer, Ears, Wrist Force and Tactile Sensor Suit; Proc. of the International Conference on Robotics and Automation, pp. 2497-2502 (1997)
- [5] I.A.Kapandji: Physiologie Articulaire; Maloine S.A. Editor (1980)
- [6] W. Pollard: Position Controlling Apparatus; U.S. Patent 2,286,571 (1942)
- [7] J.P. Trevelyan: Skills for a Shearing Robot : Dexterity and Sensing; Robotics Research, pp. 273-280 (1985)